PROCEEDINGS, Twenty-Eighth Workshop on Geothermal Reservoir Engineering
Stanford University, Stanford, California, January 27-29, 2003
SGP-TR-173

MODELING OF GEOCHEMICAL INTERACTIONS BETWEEN ACIDIC AND NEUTRAL FLUIDS IN THE ONIKOBE GEOTHERMAL RESERVOIR, JAPAN

Norifumi Todaka[1], Chitoshi Akasaka[1], Tianfu Xu[2], and Karsten Pruess[2]

1. Electric Power Development Co., Ltd., Chuo-ku, Tokyo 104-8165, Japan
e-mail: norifumi_todaka@jpower.co.jp, chitoshi_akasaka@jpower.co.jp
2. Lawrence Berkeley National Laboratory, Berkeley, CA 94720
e-mail: Tianfu_Xu@lbl.gov, K_Pruess@lbl.gov

ABSTRACT

Two types of fluids are encountered in the Onikobe geothermal reservoir, one is neutral and the other is acidic (pH=3). It is hypothesized that acidic fluid might be upwelling along a fault zone and that an impermeable barrier might be present between the acidic and neutral fluid zones. We carried out reactive geothermal transport simulations using TOUGHREACT (Xu and Pruess, 1998 and 2001) to test such a conceptual model. One-dimensional models were used to study the geochemical behavior due to mixing of the two fluids. Mn-rich smectite precipitates near the mixing front and is likely to form an impermeable barrier between regions with acidic and neutral fluids.

INTRODUCTION

Two types of fluids are encountered in the Onikobe geothermal reservoir, one is neutral and the other is acidic (pH=3). The acidic fluid is characterized by higher concentrations of Mg, Fe, Pb, Zn, and Cl compared with the neutral one. The two types of fluids are locally isolated from one another. Based on a relationship between the acidic fluid zone and acidic alteration (pyrophyllite) zone, it is determined that acidic fluid might be upwelling along the fault that forms the horst structure.

Some experience about mineral precipitation by fluid-fluid mixing has been obtained by Todaka and Tezuka (2002). Mn-rich smectite scale coexisting with sulfides armed inside some production wells by mixing of acidic and neutral fluids from two feed zones, and silica scale formed by mixing in the surface pipeline. Moreover, sphalerite and galena scales are deposited inside the production well. Reservoir fluid mixed with re-injected water might be supersaturated with respect to sphalerite and galena. In order to confirm the precipitation of these minerals by fluid-fluid mixing was simulated by the chemical equilibrium approach (Ajima *et al.*, 1998; Todaka and Tezuka, 2002) using SOLVEQ/CHILLER (Reed, 1982).

Mineral precipitation, at the mixing front of acidic and neutral fluids in the natural state and also in the exploitation (production and re-injection) stage in the reservoir, may form an impermeable barrier, resulting in changes of the overall formation permeability. Such phenomena may be the reason why acidic and neutral fluids are clearly separated in the same reservoir. Reactive chemical transport simulation was carried out to test the formation mechanism of an impermeable barrier between acidic and neutral fluid zones and to understand geochemical and hydrogeological changes due to exploitation.

NUMERICAL METHOD

Modeling of reactive geochemical transport at the Onikobe geothermal field was performed using the reactive transport computer code TOUGHREACT (Xu and Pruess, 1998 and 2001). The code uses a sequential iteration approach similar to Yeh and Tripathi (1991), Walter et al. (1994), and Xu et al. (1999), which solves the transport and reaction equations separately. Flow and transport are based on space discretization by means of integral finite differences (Narasimhan and Witherspoon, 1976). An implicit time-weighting scheme is used for the individual components of the model consisting of flow, transport, and kinetic geochemical reactions. The chemical transport equations are solved independently for each component, whereas the reaction equations are solved on a grid-block basis using Newton-Raphson iteration. Full details of the code are given in Xu and Pruess (1998 and 2001).

In the model, advective and diffusive transport of aqueous chemical species are considered. Aqueous chemical complexation is considered assuming local equilibrium. Mineral dissolution/precipitation can proceed at equilibrium and/or under kinetic conditions. Temperature effects are also considered for geochemical reaction calculations because equilibrium and kinetic data are functions of temperature.

In the present work, we neglect the following: (1) compaction and thermal mechanics, such as micro-

fracturing by thermal stress and hydro-fracturing by thermal expansion of pore fluid; (2) the effect of chemical concentration changes on fluid thermo-physical properties such as density and viscosity which are otherwise primarily dependent on pressure and temperature; (3) the enthalpy due to chemical reactions.

HYDROGEOLOGICAL AND GEOCHEMICAL CONDITIONS

Hydrogeological conditions

One-dimensional porous medium numerical models were used to verify the geochemical behavior due to mixing of acidic and neutral fluids. Schematic representations are shown in Figures 1 and 2 for the non-flow and flow models. Common rock properties in the models are as follows; grain density: 2750 kg/m^3, porosity: 0.1, permeability: 2x10^{-14} m^2, thermal conductivity: 3 W/(m°C), heat capacity: 1000 J/(kg°C). The flow model was run in isothermal as well as non-isothermal conditions. To study temperature effect, three different temperatures (230, 250 and 270°C) were considered in the isothermal flow model. The temperature range and pressure used were from field data. The number of grid blocks was increased from 10 in the non-flow model to 100 in the flow model, to show chemical reactive behavior occurring with flow in detail. Darcy velocity was set to 1 mm/day in all flow models by specification of the mass source in the left boundary block. A linear temperature gradient from 290°C to 210°C is assumed in non-isothermal flow model, to evaluate temperature effects in reactive transport.

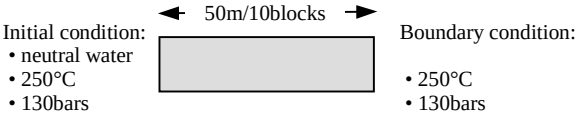

Figure. 1. Schematic representation of non-flow model.

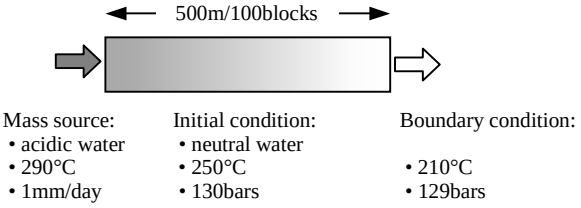

Figure. 2. Schematic representation of flow model.

Geochemical conditions

Two types of production fluids are distributed in the Onikobe geothermal reservoir. The neutral fluid has a pH of 5.5 under reservoir conditions; it is called neutral in this paper because the water at the separator is neutral in the ambient condition. Water from well 134 is selected as representative of initial water and the acidic fluid from well 130 as boundary water. Chemical concentrations of initial and boundary waters (Table 1) are calculated from separated waters (equal to re-injected water) and vapors from well 134 and well 130 using their total enthalpies.

Table. 1. Water chemical compositions used for initial and boundary conditions of the reactive chemical transport simulations.

Component	Initial water (Neutral water)	Boundary water (Acidic water)
	mole/kg	
H^{+*}	2.745E-06	3.863E-04
Cl^-	4.442E-02	9.909E-02
SO_4^{--}	6.500E-03	1.150E-02
HCO_3^-	1.372E-02	1.782E-02
SiO_2	8.498E-03	8.428E-03
Al^{+++}	5.656E-06	9.577E-06
Ca^{++}	3.098E-03	1.127E-02
Mg^{++}	5.992E-06	1.143E-03
Fe^{++}	1.491E-06	2.214E-03
K^+	3.814E-03	7.412E-03
Na^+	3.470E-02	6.228E-02
Mn^{++}	2.399E-06	5.784E-05
Zn^{++}	1.061E-07	3.376E-05
Pb^{++}	1.000E-12	5.899E-06
O_2	1.724E-40	2.344E-40
temperature (°C)	250	254
well name	134	130

*: activity

Initial mineral abundance and possible secondary minerals considered in the simulations are listed in Table 2. Possible secondary minerals were determined from field and experimental observations of water-rock interaction and from equilibrium geochemical model calculations. Calcite and anhydrite dissolution and precipitation were assumed to take place under chemical equilibrium; whereas those of the other minerals were considered under kinetic conditions. A general form of kinetic rate law (Steefel and Lasaga, 1994) is used,

$$r_m = A_m k_m \left[1 - \left(\frac{Q_m}{K_m}\right)^{\mu}\right]^n \quad (1)$$

where m is mineral index, r_m is the dissolution/precipitation rate (positive values indicate dissolution, and negative values precipitation), A_m is the specific reactive surface area per kg H_2O, k_m is the rate constant (moles per unit mineral surface area

and unit time) which is temperature dependent, K_m is the equilibrium constant for the mineral-water reaction written for the destruction of one mole of mineral m, and Q_m is the ion activity product. The parameters μ and n are positive numbers normally determined by experiment, and are usually, but not always, taken equal to unity (as in the present work). The temperature dependence of the reaction rate constant can be expressed reasonably well via an Arrhenius equation (Steefel and Lasaga, 1994). Since many rate constants are reported at 25 °C, it is convenient to approximate the rate constant dependency as a function of temperature as

$$k = k_{25} \exp\left[\frac{-E_a}{R}\left(\frac{1}{T} - \frac{1}{298.15}\right)\right] \qquad (2)$$

where E_a is the activation energy, k_{25} is the rate constant at 25 °C, R is the universal gas constant, and T is absolute temperature. Parameters k_{25} and E_a are taken from Johnson *et al.* (1998), Hardin (1998) and Tester *et al.* (1994) or estimated from data therein. The reactive surface areas of minerals used are given in the last column of Table 2.

The equilibrium constants were taken from the EQ3/6 V7.2b database (Wolery, 1992) which was derived using SUPCRT92 (Johnson *et al.*, 1992). Equilibrium constant of Mn-rich smectite was calculated based on Tardy and Garrels (1974) and Johnson *et al.* (1992). The chemical composition of Mn-rich smectite is that of smectite scale formed by fluid mixing in the production well 128 at the Onikobe geothermal field.

Table. 2. List of initial mineral volume fractions, possible secondary mineral phases, and their kinetic properties used in the simulation (k_{25} is the kinetic rate constant at 25°C, and E_a activation energy).

Mineral	Composition	Vol. Frac	k_{25} mole/(m^2S)	E_a kJ/mole	Surface area cm^2/g
Primary:					
quartz	SiO_2	0.1477	$1.04x10^{-14}$	87.70	14.77
K-feldspar	$KAlSi_3O_8$	0.0495	$1.78x10^{-12}$	36.00	4.95
albite	$NaAlSi_3O_8$	0.2232	$7.08x10^{-13}$	54.40	22.32
anorthite	$CaAl_2Si_2O_8$	0.3145	$1.50x10^{-14}$	18.40	0.01
diopside	$CaMgSi_2O_6$	0.0149	$1.00x10^{-13}$	54.40	1.49
hedenbergite	$CaFeSi_2O_6$	0.0098	$1.00x10^{-13}$	54.40	0.98
enstatite	$MgSiO_3$	0.0736	$1.00x10^{-13}$	54.40	7.26
ferrosilite	$FeSiO_3$	0.0493	$1.00x10^{-13}$	54.40	4.93
magnetite	Fe_3O_4	0.0176	$1.00x10^{-13}$	54.40	1.76
porosity		0.1			
total		1.0			
Secondary:					
clinochlore	$Mg_5Al_2Si_3O_{10}(OH)_8$	0.0	$1.00x10^{-14}$	62.76	100
daphnite	$Fe_5Al_2Si_3O_{10}(OH)_8$	0.0	$1.00x10^{-14}$	62.76	100
illite	$K_{0.6}Mg_{0.25}Al_{1.8}(Al_{0.5}Si_{3.5}O_{10}(OH)_2$	0.0	$1.00x10^{-14}$	58.62	100
kaolinite	$Al_2Si_2O_5(OH)_4$	0.0	$1.00x10^{-14}$	71.00	100
pyrophyllite	$Al_2Si_4O_{10}(OH)_2$	0.0	$1.00x10^{-14}$	71.00	100
laumontite	$CaAl_2Si_4O_{12}4H_2O$	0.0	$1.00x10^{-13}$	54.40	10
wairakite	$CaAl_2Si_4O_{12}2H_2O$	0.0	$1.00x10^{-13}$	54.40	10
prehnite	$Ca_2Al_2Si_3O_{10}(OH)_2$	0.0	$1.00x10^{-13}$	54.40	10
clinozoisite	$Ca_2Al_3Si_3O_{12}(OH)$	0.0	$1.00x10^{-13}$	54.40	10
epidote	$Ca_2Fe_3Si_3O_{12}(OH)$	0.0	$1.00x10^{-13}$	54.40	10
smectite	$(Ca_{0.17}Na_{0.01}K_{0.01})(Al_{0.18}Mg_{1.74}Mn_{0.85}Fe_{0.03})(Si_{3.87}Al_{0.13})O_{10}(OH)_2$	0.0	$1.00x10^{-14}$	58.62	100
pyrite	FeS_2	0.0	$1.00x10^{-13}$	0.00	0.001
sphalerite	ZnS	0.0	$1.00x10^{-13}$	0.00	0.001
galena	PbS	0.0	$1.00x10^{-13}$	0.00	0.001
calcite	$CaCO_3$	0.0	at equilibrium		
anhydrite	$CaSO_4$	0.0	at equilibrium		

RESULTS AND DISCUSSION

Non-flow model

Non-flow (batch) simulation was performed to study mineral assemblages and uncertain parameters such as equilibrium and kinetic conditions. Possible secondary minerals and reactive surface areas were determined by trial-and-error simulation. The non-flow simulation results in the smallest changes in chemical concentrations and precipitation/dissolution rates (mineral volume fractions) between initial and quasi-stationary state conditions.

Quasi-stationary state is reached after 10000 years. The pH increases slightly with time and then remains the same at 5.8 at 250°C after 10000 years (Figure 3). Most components except Mg, Fe, Mn and Al have almost constant concentrations. Concentrations of Mg, Fe, Mn and Al continue to change slightly before 10000 years and then remain constant. The rates of mineral dissolution and precipitation remain also constant after 10000 years (Figure 4). Consequently, there is little pH change from the initial condition. Mineral precipitation and dissolution in this simulation were almost consistent with the field data.

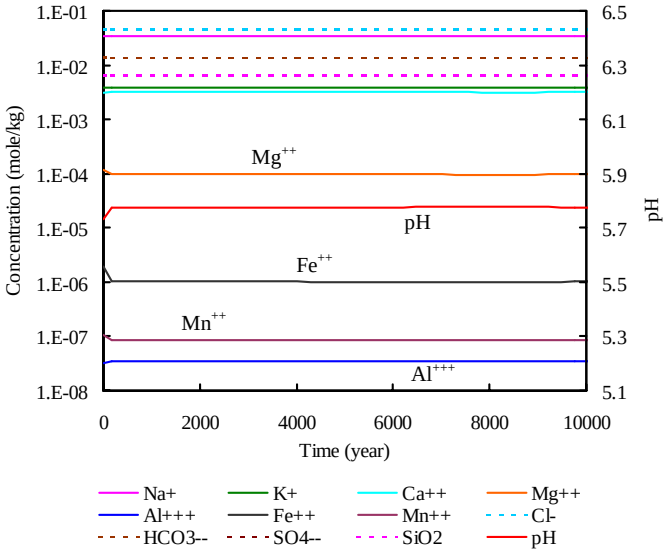

Figure. 3. Changes of pH and chemical concentrations with time in non-flow model at 250°C (center block).

Isothermal flow model

Using the parameter values determined in the non-flow simulation, the flow model was used to test precipitation and dissolution near the mixing region between acidic and neutral fluids. Concentration change of conservative chloride indicates the mixing front. The mixing front in our simulations can be seen easily due to the big difference between chloride concentrations of acidic fluid (0.099 mole/kg) and neutral fluid (0.044 mole/kg) as shown in Figure 5.

Mn-rich smectite precipitates near the mixing front, and then dissolves to disappear in the acidic flow zone at temperatures of 270 and 250°C (Figures 6 and 7). The precipitation peak of Mn-rich smectite moves downstream with time. The peak is consistent with the mixing front. The behavior of mineral precipitation and dissolution at 230°C is somewhat different from that at 250 and 270°C. At 230°C, a small amount of Mn-rich smectite dissolves by acidic fluid displaced with time (Figure 8). It is not clear why the Mn-rich smectite precipitation may occur in acidic fluid zone. This may be due to uncertain parameters.

Precipitation of pyrite, sphalerite and galena occurs in the acidic fluid zone and decrease downstream (Figure 9). Precipitation of these sulfides increases with temperature decreasing. This is because sulfide solubility increases with decreasing temperature. Sulfide precipitation does not obviously occur near the mixing front in these isothermal flow simulations.

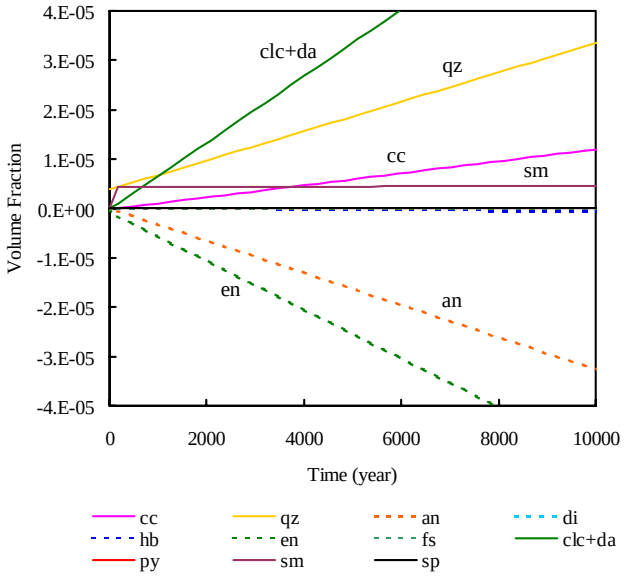

Figure. 4. Changes of mineral abundance (in volume fraction) with time in non-flow model at 250°C (center block). cc: calcite, qz: quartz, an: anorthite, di: diopside, hb: hedenbergite, en: enstatite, fs: ferrosilite, clc: clinochlore, da: daphnite, py: pyrite, sm: Mn-rich smectite, sp: sphalerite

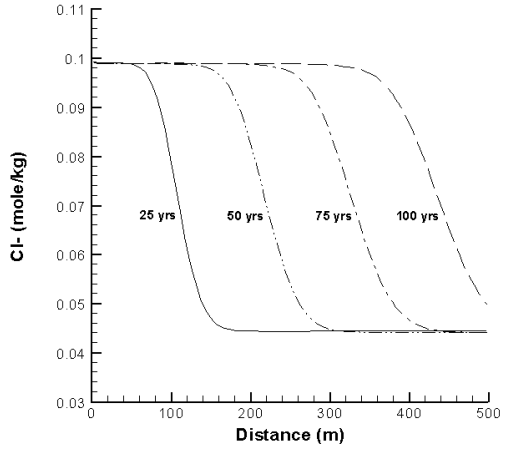

Figure. 5. Cl^- concentration in One-dimensional flow model at 230°C.

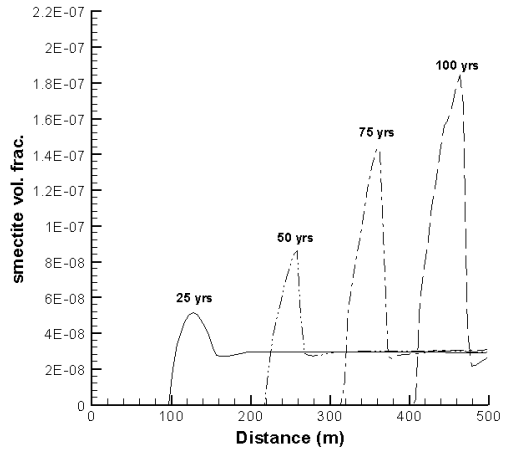

Figure. 6. Changes of Mn-rich smectite volume fraction in the flow model at 270°C.

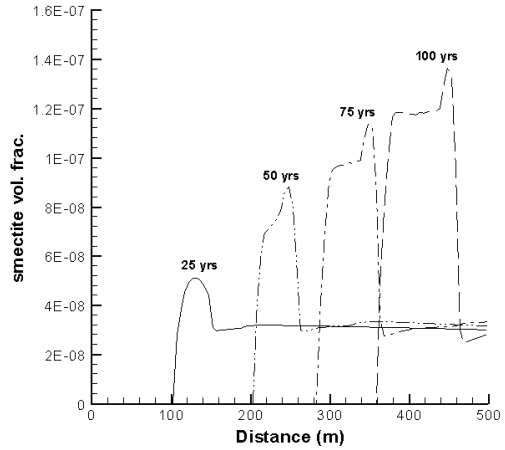

Figure. 7. Changes of Mn-rich smectite volume fraction in the flow model at 250°C.

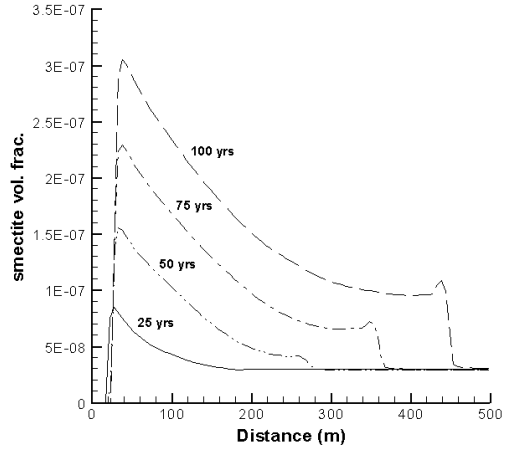

Figure. 8. Changes of Mn-rich smectite volume fraction in the flow model at 230°C.

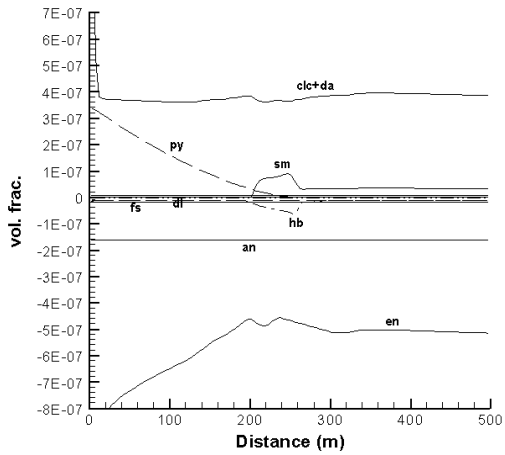

Figure. 9. Changes of mineral volume fraction in the isothermal flow model after 50 years at 250°C. Abbreviations are as in Figure 4.

Non-isothermal flow model

The chloride concentration (Figure 10) in the non-isothermal flow model runs almost parallel. A big change of pH due to the movement of the mixing front gradually slows down with time, compared with that of chloride (Figure 11).

Mn-rich smectite precipitates near the mixing front, and then dissolves by acidic water displaced with time due to the pH decrease. The movement of the Mn-rich smectite peak (Figure 12) is similar to that of pH, and is behind that of Cl. At the lower temperature, the peak is much higher. Precipitation of pyrite, sphalerite and galena occurs near the mixing front, and their precipitation peaks move with the mixing front (Figures 13-15). Mn-rich smectite scale in the Onikobe production well also coexists with sphalerite and galena (Ajima *et al.*, 1998). The mineral assemblage of the scale is the same as that found in this simulation. It

is likely that this smectite will precipitate by fluid mixing in the Onikobe reservoir.

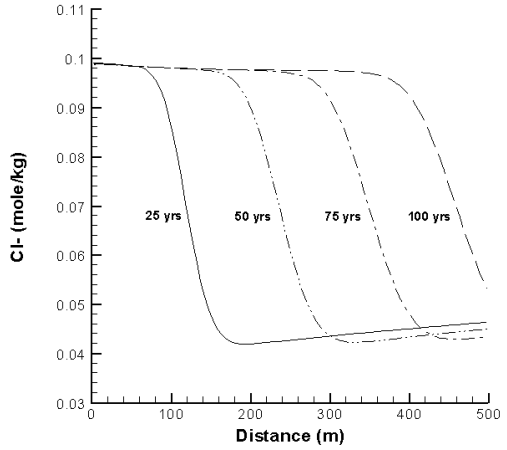

Figure. 10. Cl concentration in the non-isothermal model.

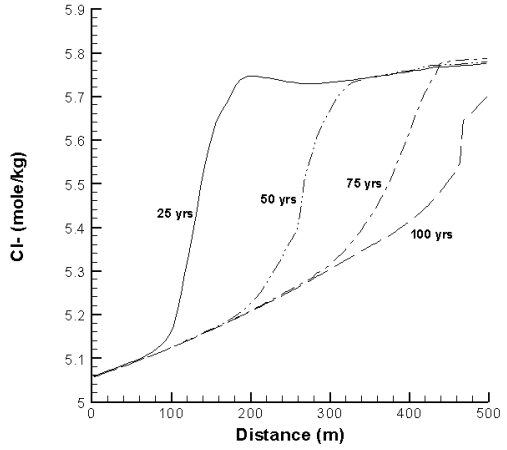

Figure. 11. Water pH in the non-isothermal model.

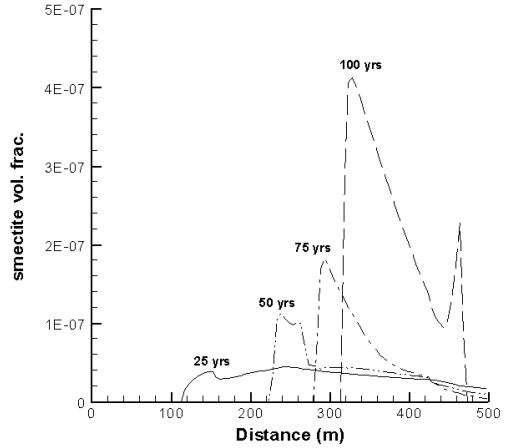

Figure. 12. Changes of Mn-rich smectite volume fraction in the non-isothermal model.

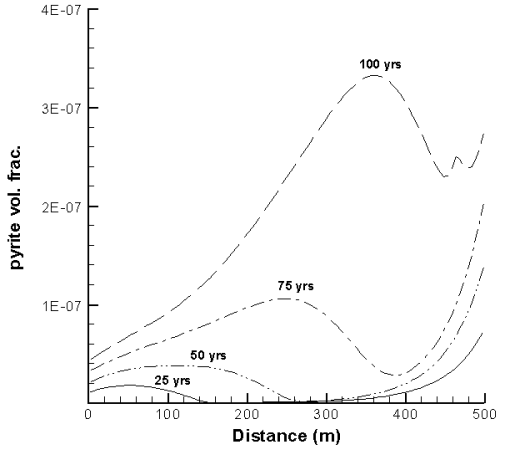

Figure. 13. Changes of pyrite volume fraction in the non-isothermal model.

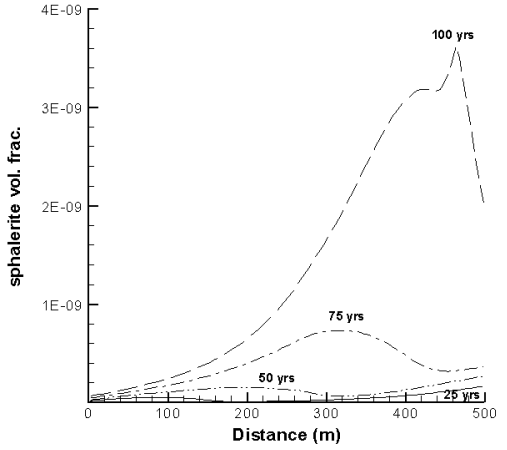

Figure. 14. Changes of sphalerite volume fraction in the non-isothermal model.

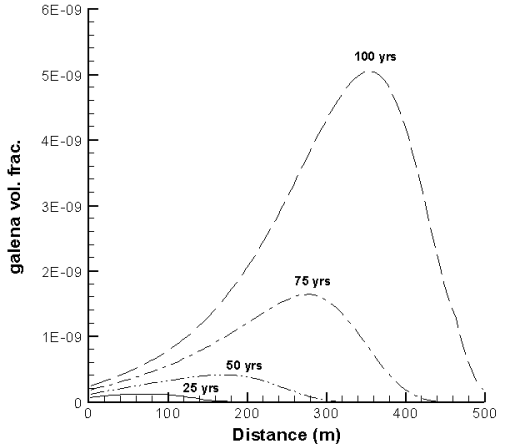

Figure. 15. Changes of galena volume fraction in the non-isothermal model.

The most important mineralization is not only hydrothermal metasomatism (chlorite, illite, kaolinite, epidote etc. form by replacement of primary minerals in rocks), but mineral deposition (quartz, calcite, anhydrite precipitates from geothermal fluid in fractures). Quartz, calcite and pyrite form by both formation mechanisms. Mn-rich smectite precipitation is observed at a depth where neutral fluid encountered with acidic fluid rising from deep feed zone in the Onikobe production wells (Ajima *et al*., 1998). It is assumed that this smectite is not formed by replacement of primary minerals but precipitates by mixing of two different types of fluids in open fractures. Precipitation of Mn-rich smectite has an effect on decreasing porosity and permeability, and it is likely to form an impermeable barrier between regions with acidic and neutral fluids for geologic time.

Sensitivity to the reactive surface area

For the purpose of analyzing sensitivity to reaction kinetic rates, we performed two additional non-isothermal flow simulations by increasing and decreasing the surface areas listed in Table 2 by one order of magnitude, respectively. These analyses can give some understanding of the behavior of Mn-rich smectite precipitation affected by reaction kinetic rates. Figure 12 shows changes of Mn-rich smectite volume fraction using the surface areas as listed in Table 2. The result obtained by decreasing the surface areas by one order of magnitude is presented in Figure 16. The pattern of Mn-rich smectite precipitation is very close to that of the base case (Figures 12). For the simulation with the surface area increasing, the result of Mn-rich smectite is presented in Figure 17. The pattern and magnitude are different from the previous two simulations, and the peak movement is slower. Nevertheless, the precipitation peak in all three cases moves downstream with time.

CONCLUSION

One-dimensional simulations (isothermal and non-isothermal flow simulations) were performed for geothermal interactions between acidic and neutral fluids in the Onikobe geothermal reservoir using the reactive geochemical transport simulator TOUGHREACT. The results of isothermal and non-isothermal simulations are generally consistent. Mn-rich smectite precipitates near the mixing front, and then dissolves to disappear in the acidic flow zone at higher temperature. Mn-rich smectite does not dissolve by the acidic water at lower temperature.

Mn-rich smectite precipitation/dissolution relates to pH and temperature. Precipitation of sphalerite and galena occurs in a similar region as the Mn-rich smectite precipitation. Mn-rich smectite coexists with sphalerite and galena. It is assumed that these minerals are not formed by mineral replacement but by mineral deposition due to mixing of two different types of fluids in open fractures. The smectite precipitation is likely to fill up open fractures and to form an impermeable barrier between regions with acidic and neutral fluids during geologic time.

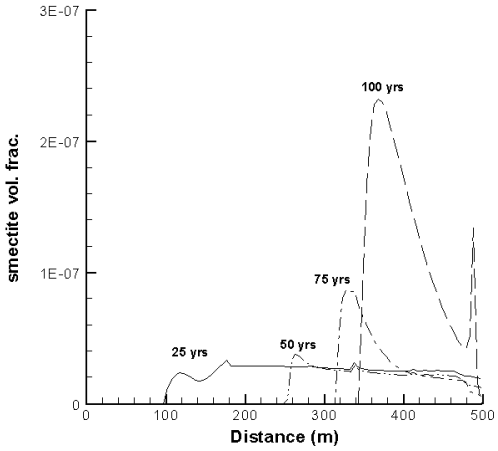

Figure. 16. Changes of Mn-rich smectite volume fraction obtained by decreasing surface areas by one order of magnitude in the non-isothermal model.

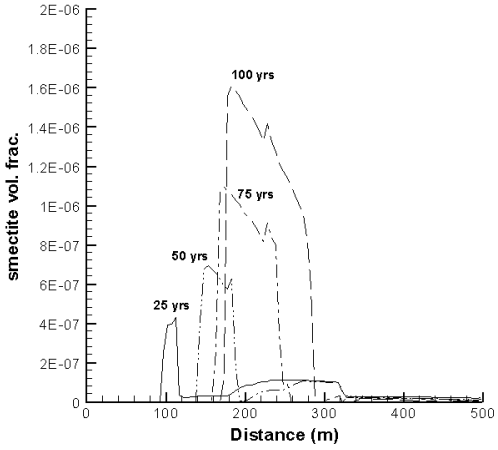

Figure. 17. Changes of Mn-rich smectite volume fraction obtained by increasing surface areas by one order of magnitude in the non-isothermal model.

The present simulation results are specific to the reservoir conditions and parameters considered, and water and mineral compositions used in this study. Precipitation/dissolution of minerals is quite consistent with those of the Onikobe field data. However, some minerals does not precipitate in this simulation even if these minerals are generally observed at the Onikobe field. There are numerous uncertainties such as the chemical kinetics and the lack of sufficiently detailed characterization data at the Onikobe field. Further simulations will be performed by increasing or

decreasing the surface areas and by adjusting mineral assemblages, and then two-dimensional simulation will be carried out to confirm the results of one-dimensional models.

ACKNOWLEDGEMENTS

This work was supported by a project provided Electric Power Development Co., Ltd. (Japan), and by the Director, Office of Science, Office of Basic Energy Sciences, of U.S. Department of Energy, under Contract No. DE-AC03-76SF00098 with Lawrence Berkeley National Laboratory. We are grateful to Eric Sonnenthal and Curtis Oldenburg for a review of the manuscript.

REFERENCES

Ajima, S., Todaka, N., and Murakake, H. (1998), "An interpretation of smectite precipitation in production wells caused by the mixing of different geothermal fluids", *Proc. Twenty-third Workshop on Geothermal Reservoir Engineering*, Stanford Univ., 264-269.

Hardin, E. L. (1998), "Near-field/altered zone models, Milestone report for the CRWMS M&O", U.S.Department of Energy, SP3100M4: Livermore, California, Lawrence Livermore National Laboratory.

Johnson, J. W., Knauss, K. G., Glassley, W. E., Deloach, L. D. and Tompson, A. F. B. (1998), "Reactive transport modeling of plug-flow reactor experiments: Quartz and tuff dissolution at 240ºC", *Jour. Hydrol.*, **209**, 81-111.

Johnson, J. W., Oelkers, E. H., and Helgeson, H. C. (1992), "SUPCRT92: A software package for calculating the standard molal thermodynamic properties of minerals, gases, aqueous species, and reactions from 1 to 5000 bars and 0 to 1000 degrees C", *Computers and Geosciences*, **18**, 899-947.

Narasimhan, T. N. and Witherspoon, P. A. (1976), "An integrated finite difference method for analyzing fluid flow in porous media", *Water Resour. Res.*, **12**, 57-64.

Reed, M. H. (1982), "Calculation of multicomponent chemical equilibria and reaction processes in systems involving minerals, gases and an aqueous phases", *Geochim. Cosmochim. Acta*, **46**, 513-528.

Steefel, C. I., and Lasaga, A. C., (1994), "A coupled model for transport of multiple chemical species and kinetic precipitation/dissolution reactions with applications to reactive flow in single phase hydrothermal system", *Amer. Jour. Sci*., **294**, 529-592.

Tardy, Y. and Garrels, R. M. (1974), "A method of estimating the Gibbs energies of formation of layer silicates", *Geochim. Cosmochim. Acta*, **38**, 1101-1116.

Tester, J. W., Worley, W. G., Robinson, B. A., Grigsby, C. O. and Feerer, J. L. (1994), "Correlating quartz dissolution kinetics in pure water fom 25 to 625ºC", *Geochim. Cosmochim. Acta*, **58**, 2407-2420.

Todaka, N and Tezuka, S. (2002), "Utilization of geochemistry for maintenance of geothermal power plant. Water-dominated reservoir: Onikobe geothermal power plant (Geochemistry for geothermal development)", *Chinetsu*, **39**, 60-71 (in Japanese).

Walter, A. L., Frind, E. O., Blowes, D. W., Ptacek, C. J., Molson, J. W. (1994), "Modeling of multicomponent reactive transport in groundwater: 1, Model development and evaluation", *Water Resour. Res.*, **30**, 3137-3148.

Wolery, T. J. (1992), EQ3/6: "Software package for geochemical modeling of aqueous systems: Package overview and installation guide (version 7.0)", Lawrence Livermore National Laboratory Report UCRL-MA-110662 PT I, Livermore, California.

Xu, T. and Pruess, K. (1998), "Coupled modeling of non-isothermal multi-phase flow, solute transport and reactive chemistry in porous and fractured media: 1. Model development and validation", Lawrence Lawrence Berkeley National Laboratory Report LBNL-42050, Berkeley, California.

Xu, T. and Pruess, K. (2001), "Modeling multiphase non-isothermal fluid flow and reactive geochemical transport in variability saturated fractured rocks: Methodology" *Amer. Jour. Science*, **301**, 16-33.

Xu, T., Samper, J., Ayora, C., Manzano, M., and Custodio, E., (1999), "Modeling of non-isothermal multi-component reactive transport in field-scale porous media flow system", *Jour. Hydrol*., **214**, 144-164.

Yeh, G. T. and Tripathi, V. S. (1991), "A model for simulating transport of reactive multispecies components: model development and demonstration", *Water Resour. Res.*, **27**, 3075-3094.